JOURNAL OF VIROLOGY, Aug. 1979, p. 447-462
0022-538X/79/08-0447/16$02.00/0

Vol. 31, No. 2

Isolation and Localization of Herpes Simplex Virus Type 1 mRNA Abundant Before Viral DNA Synthesis

LOUIS E. HOLLAND, KEVIN P. ANDERSON, JAMES R. STRINGER,† AND EDWARD K. WAGNER*

Department of Molecular Biology and Biochemistry, University of California, Irvine, Irvine, California 92717

Received for publication 12 January 1979

Herpes simplex virus type 1 (HSV-1) DNA covalently bound to cellulose was used as a reagent to isolate viral RNA transcripts for size analysis on denaturing agarose gels. Nuclear and polyribosomal RNA isolated at 2 h postinfection (p.i.) migrated with sizes between 1,500 and 5,500 nucleotides. At 6 h p.i. (when viral DNA synthesis is underway), viral polyribosome-associated polyadenylated RNA showed different discrete sizes of species predominating, with RNA larger than 5,500 nucleotides clearly present. Nearly 50% of the newly made viral RNA found in the nucleus at 6 h p.i. was from 5,000 to 10,000 nucleotides in length. A high-resolution transcription map of the viral mRNA abundant at 2 h p.i. was compiled from the hybridization of Southern blots of HSV-1 DNA restriction fragments to both sizes of fractionated polyribosomal polyadenylated RNA and 3′ complementary DNA probe made to this size of fractionated RNA. We have identified and mapped 16 mRNA species abundant at 2 h p.i. These RNAs range in size from 1,500 to 5,300 nucleotides and map throughout the HSV-1 genome. In some instances, a direction of transcription can be suggested. Further, about one-third of this number of mRNA's has been found in cells infected with a DNA-negative temperature-sensitive mutant (*ts*B2) and grown at the nonpermissive temperature (39°C).

Herpes simplex virus type 1 (HSV-1) contains a linear, double-stranded DNA genome of 95×10^6 to 100×10^6 daltons (d) (11, 34). Lower values for the molecular weight previously reported by this laboratory (36, 37) were based on values for T4 and φX replicative-form II (φXRFII) DNA accepted at that time, but which now are known to be significantly below the actual values. Regardless, the strain of HSV-1 we are using (KOS) has an electron microscopic contour length of 28.1 times that of φXRFII (36) so that it is 150,000 base pairs (150 kilobase [kb] pairs) in length, based on the known length of the standard (25). The viral DNA has been shown to be structurally complex and consists of a long and a short region, each composed of unique sequences that are bounded by different inversely repeated sequences (34). These two regions have been found to orient themselves such that four equimolar configurations of the viral DNA are obtained (12, 40).

We and other workers have been investigating the properties of HSV-1 mRNA. Viral mRNA shares general properties with host cell mRNA; i.e., it is synthesized in the nucleus (35), polyadenylated on the 3′ end (2, 26, 28), and capped on the 5′ end (4, 20). The abundant HSV-1 mRNA species appearing before the onset of viral DNA synthesis (early—the times after infection used in this paper) can be differentiated into two classes. One class, representing 10 to 15% of the genome, consists of the immediate early, or α, mRNA's which are found in high abundance in the cytoplasm of cells treated with cycloheximide from the time of infection (16). Jones et al. (15), using RNA excess solution hybridizations, and Clements et al. (6), using Southern-blot hybridizations, have shown that the α mRNA species map in specific, noncontiguous sites on the HSV-1 genome. The other major abundant class of mRNA species found before viral DNA replication are the β messages. These mRNA's encode proteins which are synthesized after proteins encoded by the α mRNA species have been synthesized (14). Together, the α and β mRNA's represent approximately 25% of the HSV-1 DNA sequences (16, 31, 33). Stringer et al. (29) used electron microscopy to show that although these α and β mRNA species map throughout the HSV-1 genome, they hybridize more frequently to some regions than to others.

By 6 h postinfection (p.i.), when viral DNA

† Present address: Cold Spring Harbor Laboratory, Cold Spring Harbor, NY 11724.

synthesis is maximal, the majority of the early RNA sequences continue to be synthesized, and transcripts from an additional 20% of the viral genome are found in good yield on polyribosomes (28). The additional RNA comprises γ, or true late mRNA species, and is present at about one-fifth the concentration of the α and β messages. RNA sequences homologous to γ mRNA have been detected even at the earliest times after infection, but then at a 10- to 20-fold-lower concentration than the α and β mRNA (16, 31).

We previously have reported methods for the isolation and characterization of total HSV-1 mRNA synthesized after viral DNA replication (1). On the basis of our preliminary data, we can identify more than 30 discrete viral mRNA species ranging in size from greater than 8,000 to at least 1,500 nucleotides (>8 to 1.5 kb) in length. These viral mRNA species map throughout the HSV-1 genome; however, abundant amounts of species larger than 4 kb are found only in the long unique region. Also, certain small areas of the viral genome encode a number of mRNA species, suggesting that some HSV-1 mRNA species have overlapping sequences.

In the experiments reported in this paper, we have examined the readily resolvable, abundant HSV-1 mRNA synthesized early after infection. This RNA has a size distribution from 5.5 to 1.5 kb, although small amounts of larger species can be detected. We have used Southern-blot hybridization of HSV-1 DNA restriction fragments to size fractionated, early polyribosomal RNA to identify and map a minimum of 16 abundant early mRNA species. On the basis of size of each of these, species can be correlated with an mRNA species previously mapped late in the same location.

Further, we have identified about one-third of the number of mRNA species as being produced at nonpermissive temperatures after infection with a DNA-negative, temperature-sensitive (*ts*) mutant of HSV-1 (*ts*B2).

MATERIALS AND METHODS

Cells and virus. Monolayer cultures of HeLa cells were grown in Eagle minimum essential medium with Earle salts, 10% calf serum, and no antibiotics. Growth conditions and assay for mycoplasmic contamination were as previously described (30). Stocks of the KOS strain of HSV-1 were grown in HeLa cells at a multiplicity of 0.1 PFU/cell and prepared as described previously (36). The KOS mutant strain *ts*B2 was obtained from P. Schaffer at the Harvard Medical School and was not passaged before use.

Isolation, labeling, and fractionation of RNA. Cells were infected at a multiplicity of 10 PFU/cell for 30 min at 37°C in phosphate-buffered saline (9) containing 0.1% fetal calf serum and then overlaid with medium 199 containing 5% fetal calf serum. Time after infection was measured after the absorption period. For preparation of polyribosomal RNA, cells were lysed in buffer containing 25 mM Tris (pH 7.5), 25 mM NaCl, 5 mM $MgCl_2$, 50 μg of heparin per ml, 5% sucrose, and 2% Triton X-100. The polyribosome-associated RNA was isolated by the Mg^{2+} precipitation method of Palmiter (22) as described previously (28). The precipitated polyribosomes were suspended in 100 mM NaCl-10 mM Tris-5 mM EDTA-0.5% sodium dodecyl sulfate (pH 7.4), digested with 250 μg of Proteinase K (Merck & Co., Inc.) per ml for 15 min at 45°C, gently extracted with phenol and chloroform (28), and precipitated with 2 volumes of ethanol at −20°C. Polyadenylated [poly(A)] RNA was obtained by use of oligodeoxythymidylic acid (oligo[dT])-cellulose (Collaborative Research, Inc. [10]).

Nuclei were isolated from cells lysed in 10 mM NaCl-10 mM Tris-1.5 mM $MgCl_2$ (pH 7.4) (reticulocyte standard buffer [RSB]), containing 0.5% Nonidet P-40 (Shell). These nuclei were then ruptured in 500 mM NaCl-10 mM Tris-50 mM $MgCl_2$ (pH 7.4) and briefly digested with 200 μg of electrophoretically purified DNase (Sigma Chemical Co.) at 37°C. A 0.1 volume of 250 mM EDTA (pH 7.5) and a 0.05 volume of 10% sodium dodecyl sulfate were added, and the nuclear lysate was digested with proteinase K and extracted as described above.

Tritium-labeled RNA was isolated as above from cells overlaid at 1.5 h p.i. for 45 min with 180 μCi of [^{3}H]uridine (28 Ci/mmol, Schwarz/Mann) per 2×10^7 cells (T-150 flask) in 12 ml of medium 199 containing 5% fetal calf serum which had been dialyzed against sterile 0.15 M NaCl. For ^{32}P-labeled RNA, cells were overlaid with 2 to 4 mCi of $^{32}P_i$ (New England Nuclear Corp.) per T-150 flask in 12 ml of Eagle minimum essential medium containing 1/10 the normal phosphate level and 5% dialyzed fetal calf serum. Labeling time was from 0 to 2 h p.i.

Size fractionation of labeled RNA was achieved by electrophoresis on 1.2% agarose (Sigma) gels containing 10 mM methylmercury hydroxide (Alpha-Ventron). These gels are completely denaturing, and the migration is linearly related to the log RNA size for the size ranges studied (3, 13). All procedures involving CH_3HgOH were performed in a ventilated hood, and protective gloves were worn at all times. ^{32}P-labeled rRNA prepared as previously described from HeLa cells (28) was included as an internal standard for ^{3}H-labeled samples and in parallel gels for ^{32}P-labeled samples. After electrophoresis, the gels were soaked in 50 mM β-mercaptoethanol for 20 min and sliced at 2- or 3-mm intervals. Tritium radioactivity in each slice was measured by dissolving slices in 0.3 ml of 7% perchloric acid at 78°C and mixing with 4 ml of Aquasol II (New England Nuclear Corp.) Radioactivity from ^{32}P-labeled RNA gels was determined by Cerenkov radiation counting of the intact slices.

Isolation of HSV DNA. Cells grown in plastic roller bottles (10^8 cells per bottle) were infected with a multiplicity of 10 PFU/cell and incubated in medium 199 containing 5% fetal calf serum. At 20 h p.i., supernatant virions from the cell overlay medium and cytoplasmic virions were collected as follows: the overlay

medium was poured off and stored on ice; the cells were scraped into ice-cold 0.15 M NaCl and pelleted by spinning at 1,000 × *g* for 5 min. The cell pellet was suspended in RSB containing 0.5% Nonidet P-40 for 10 min on ice. The saline supernatant was added to the overlay medium, and this was centrifuged at 6,000 × *g* for 10 min to pellet floating cells. This material was pooled with the bulk of the cells and lysed with 10 strokes of a tight-fitting glass Dounce homogenizer, followed by centrifugation at 8,000 × *g* for 8 min. HSV in the cell lysate supernatant was pooled with the medium supernatant and pelleted by centrifugation at 27,000 × *g* for 20 min. All centrifugations were performed at 0 to 4°C. The virus-containing pellet was resuspended in a small volume of 100 mM NaCl–10 mM HEPES (*N*-2-hydroxyethylpiperazine-*N'*-2-ethanesulfonic acid)–20 mM EDTA (pH 7.4), gently lysed by the addition of 0.1 volume of 20% Sarkosyl and 0.05 volume of 10% sodium dodecyl sulfate, and digested with 300 μg of proteinase K per ml for 3 h at 45°C. Viral DNA was purified by a single cycle of isopycnic centrifugation as described previously (37).

Restriction enzyme digestion and fragment purification. The restriction enzymes used in these studies were *Bgl*II, *Hin*dIII, and *Xba*I from New England Biolabs and *Hpa*I from Bethesda Research Laboratories. All digestions were performed under conditions recommended by the supplier. Amounts of 1 to 3 μg of restricted DNA were electrophoresed on 0.5% agarose gels (0.6 by 14 cm) in 40 mM Tris–5 mM sodium acetate–2 mM EDTA (pH 7.8) at 1 mA/gel (2 V/cm) for 24 h at room temperature. Alternatively, restriction fragments were separated by electrophoresis on horizontal slabs (42 by 20 by 1.2 cm) of 0.5% agarose for 48 h at 70 mA (1.2 V/cm). Bands were visualized by UV fluorescence of ethidium bromide-stained DNA.

Bands containing restriction fragments were cut from the gel and recovered by binding to hydroxylapatite columns and eluting in 0.5 M phosphate buffer (17). The DNA then was extracted overnight with isopentyl alcohol saturated with 10 mM EDTA, desalted by passage through a column (1 by 30 cm) of Sephadex G-25 equilibrated in 100 mM NaCl–10 mM Tris–1 mM EDTA (pH 7.4), and stored at −20°C.

Preparation of HSV DNA bound to cellulose. HSV DNA was bound to diazotized cellulose, using a modification of the Noyes and Stark method (21) as described by Anderson et al. (1). Briefly, DNA was precipitated with 2 volumes of ethanol and pelleted at 20,000 × *g*. The DNA was suspended in 80% dimethyl sulfoxide–2 mM potassium phosphate (pH 6.5) and heated to 78°C for 5 min before coupling to assure complete denaturation. Cellulose was diazotized as described by Noyes and Stark (21). After coupling at 4°C for 48 h, the cellulose suspension was rinsed twice with 80% dimethyl sulfoxide–2 mM KPO_4 (pH 6.5) at 50°C, four times with 0.1× SSC (SSC is 150 mM NaCl plus 15 mM trisodium citrate) at 25°C, three times with 98% formamide–10 mM HEPES (pH 8.0), and three times with hybridization buffer (400 mM Na^+, 100 mM HEPES [pH 8.0], 5 mM EDTA) containing 80% formamide and stored in formamide hybridization buffer under nitrogen at 4°C. Small amounts of ^{32}P-labeled viral DNA, included in each reaction as a measure of the coupling efficiency, routinely showed 35 to 45% of the input DNA remaining coupled after rinsing.

HSV DNA:RNA hybridization in the absence of DNA reannealing. RNA-to-DNA cellulose hybridizations were done under conditions in which HSV DNA will not reanneal. As shown by Casey and Davidson (5), in high levels of formamide, RNA:DNA hybrids form at incubation temperatures near the melting temperature of the DNA duplex, where there is no DNA:DNA reassociation. Under our conditions of hybridization (400 mM Na^+, 80% formamide), we have established that the melting temperature for HSV-1 DNA is 62°C, that the optimum incubation temperature for RNA:DNA hybrid formation is 57°C, and that at 57°C no detectable DNA:DNA reannealing occurs.

Hybridization of RNA to DNA cellulose. Hybridizations to DNA cellulose were carried out using 0.5×10^6 to 1×10^6 ^3H cpm of RNA and 8 to 12 μg of HSV DNA coupled to 1 mg of cellulose. Hybridization was for 4 h at 57°C. After incubation, unhybridized RNA was removed by extensive rinsing in 2× SSC, followed by hybridization buffer at room temperature and finally by hybridization buffer at 60°C. Hybridized RNA was eluted with 98% formamide containing 10 mM HEPES (pH 8) at 60°C. The eluant was adjusted to 100 mM sodium acetate and 20% formamide, and the RNA was collected by ethanol precipitation and centrifugation.

DNA Southern-blot hybridization of size-fractionated RNA. Restriction endonuclease-digested HSV-1 DNA was transferred from agarose gels to nitrocellulose paper (BA85, Schleicher & Schuell Co.) by the method of Southern (27). These DNA blots were used for hybridization of ^{32}P-labeled RNA from individual slices of methylmercury-agarose gels. Gel slices were dissolved in hybridization buffer containing 65% formamide by heating at 78°C for 5 min. The RNA samples and the nitrocellulose DNA blots were sealed in plastic bags and hybridized at 57°C for 48 h. After hybridization, the nitrocellulose strips were given three 1-h rinses in 65% formamide–2.1× SSC at 45°C. They then were wrapped in Saran Wrap and pressed next to Kodak X-Omat-R X-ray film for 1 to 7 days, in some cases using photosensitizing screens (Cronex Lighting Plus, DuPont Co. [32]).

Preparation and hybridization of HSV RNA 3' probe cDNA. RNA was labeled with 10% of the normal amount of ^{32}P and polyribosomal poly(A) RNA isolated at 2 h p.i. This RNA was fractionated on methylmercury-agarose gels; the gels then were soaked, sliced, and counted as described above. Slices of the gels containing RNA of interest were incubated for 30 min with 100 mM NaOH at room temperature to degrade the RNA to an average size of 400 to 500 nucleotides in length. This was determined by treating a control slice containing ^{32}P-labeled 28S rRNA in the same manner and then eluting and electrophoretically sizing this material on a denaturing agarose gel. The gel slices were neutralized by addition of HCl and minced in 500 mM NaCl–10 mM Tris–1 mM EDTA, pH 7.6. RNA was eluted by soaking overnight, agarose

was removed by centrifugation, and the supernatant RNA was passed through an oligo(dT)-cellulose column. Poly(A)-containing RNA was eluted with 10 mM Tris-1 mM EDTA, pH 7.6; the eluant was adjusted to 100 mM sodium acetate, and the poly(A)-containing RNA was precipitated with ethanol. The RNA pellet was suspended in 0.1 ml of buffer containing 50 mM Tris (pH 8.1), 8 mM $MgCl_2$, 50 mM KCl, 0.4 mM dATP, dGTP, and dCTP, 4 mM dithiothreitol, 100 μg of actinomycin D per ml, 50 μCi of [^{32}P]TTP (350 Ci/mmol, Amersham Corp.), and 1 to 3 μg of oligo-$(dT)_{12-18}$ (Collaborative Research, Inc.) per ml. Ten units of avian myeloblastosis virus reverse transcriptase (a gift from D. Temeier) was added, and the sample was incubated at 37°C for 60 min. The reaction was stopped by adding 0.05 volume of 10% sodium dodecyl sulfate and 0.1 volume of 0.25 M EDTA. The mix then was digested with 100 μg of proteinase K per ml for 20 min at 45°C and loaded onto a Sephadex G-50 column equilibrated in 100 mM NaCl-10 mM Tris (pH 7.4)-5 mM EDTA. The excluded radioactivity was phenol chloroform extracted and RNA hydrolyzed overnight in 0.3 M NaOH. The solution was neutralized with acetic acid, and the complementary DNA (cDNA) was ethanol precipitated. The 3′ probe cDNA made in this way has a size range of <100 to ~10 nucleotides as determined by electrophoresis on denaturing agarose gels. The weight average size is 15 to 20 nucleotides, based on the relative amounts of radioactivity migrating at different sizes in the 10- to 100-nucleotide range.

Hybridization of cDNA to Southern blots was carried out for 48 h at 45°C in 65% formamide containing hybridization buffer and Denhardt solution (0.02% Ficoll, 0.02% polyvinylpyrollidone, 0.02% bovine serum albumin [8]). Blots were incubated in this buffer for 4 h at 45°C before the addition of the cDNA samples. After hybridization, the DNA blots were rinsed and subjected to autoradiography.

RESULTS

Size range of HSV-1 RNA synthesized before viral DNA synthesis. We have demonstrated elsewhere that HSV DNA bound to cellulose is a highly specific reagent for isolating viral RNA (1). Controls using uninfected cell RNA or bacterial DNA bound to cellulose show that nonspecific background is 0.05 to 0.1% of added radioactivity. Further, no nicking of ^{32}P-labeled marker RNA can be demonstrated under our hybridization conditions. We isolated polyribosomal poly(A) RNA and total nuclear RNA from 4×10^7 HSV-1-infected cells labeled from 1.5 to 2.25 h p.i. with [^{3}H]uridine. This RNA was hybridized to HSV DNA cellulose and fractionated by denaturing agarose gel electrophoresis (Fig. 1A and B). It can be seen that at this time after infection, viral polyribosomal poly(A) RNA and nuclear RNA have the same size distribution, the bulk of radioactivity migrating in sizes between 1.5 and 5.4 kb. These sizes were determined from the migration rates of individual bands of radioactivity compared with the migration of 28S (1.76×10^6 d; 5.2 kb [18, 39]) and 18S (0.67×10^6 d; 2 kb [18, 39]) ^{32}P-labeled HeLa cell rRNA included as a size marker. As we have described previously (13), Bailey and Davidson (3) showed that electrophoresis on the denaturing agarose gels used in these experiments separates RNA as a linear function of the log of its size.

The size distribution of HSV-specific polyribosomal poly(A) and nuclear RNA from cells labeled from 5.26 to 6 h p.i. is shown in Fig. 1C and D. At this time after infection, there was a shift in the proportion of radioactivity found in certain sizes of ribosomal poly(A) RNA. The proportion of labeled viral RNA migrating at >5.2 kb and between 3 and 4 kb increased, and radioactive viral RNA of a size between 1.8 and 2 kb, although still a major component of the total, was no longer predominant. In the nucleus at 6 h p.i., radioactivity in RNA larger than 5 kb accounted for 40 to 50% of all of the nuclear viral RNA labeled in the pulse, and the distribution of radioactivity was quite different from that seen in polyribosomes. This was in marked contrast to the situation at 2 h p.i.; however, as with the earlier time, the actual size range of viral nuclear RNA was similar to that seen on polyribosomes (>9 to >1 kb).

Comparisons between the relative amount of radioactivity seen in a given size range of viral RNA is valid only if hybridization is under conditions of sufficient DNA excess that all RNA populations are representative. We carried out two types of control experiments to demonstrate that this was, in fact, the case. In the first, polyribosomal poly(A) RNA labeled from 5.25 to 6 h p.i. was hybridized with DNA cellulose at one-fifth and twice the concentrations used in the experiments described; in both cases, the relative proportion of radioactivity in RNA of all sizes was the same as under our standard conditions (data not shown). Second, we took a portion (before hybridization) of the polyribosomal poly(A) RNA used in the experiment of Fig. 1A and fractionated it on a denaturing agarose gel. The gel was then sliced, and each slice was hybridized to excess HSV DNA in solution. Both the size distribution and relative amounts of viral RNA of all sizes determined in this way were identical to those found with DNA cellulose (Fig. 1E). Taken together, these experiments demonstrate that the population of viral RNA seen by using DNA cellulose as a reagent for isolation was truly representative of the viral RNA in the cell. The experiment of Fig. 1E further shows that there was no degradation of viral RNA during the preparative hybridization.

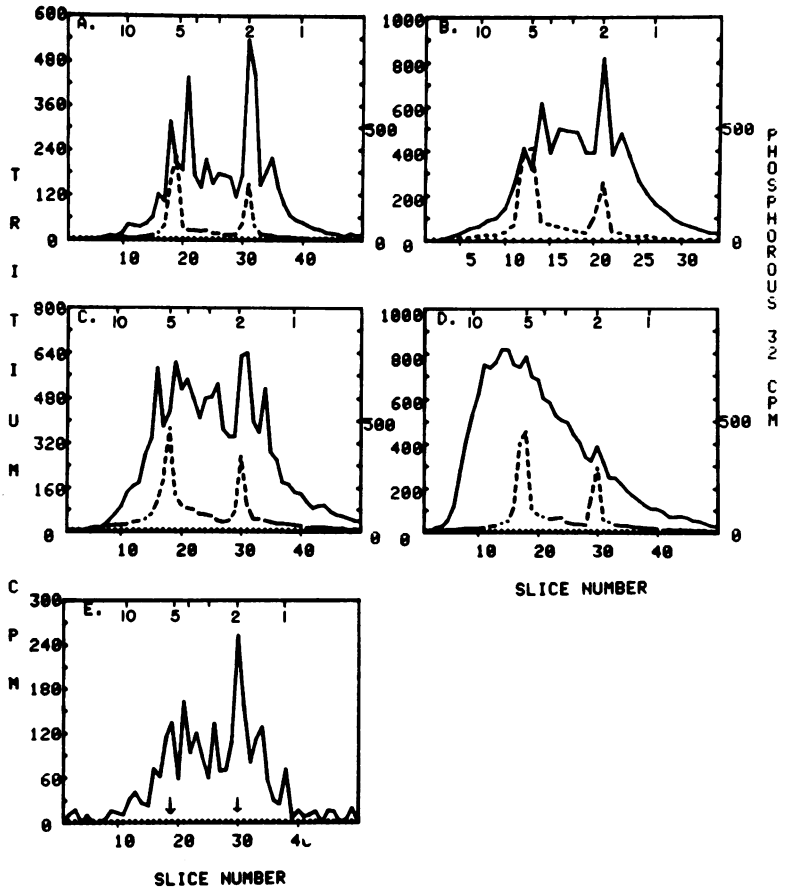

FIG. 1. *Size distribution of HSV-1 transcripts. Infected cells, pulsed with [^{3}H]uridine for 45 min, were fractionated into nuclei and polyribosomes. The RNA was extracted, hybridized to HSV-1 DNA bound to cellulose, and electrophoresed on methylmercury-agarose gels. (A) Viral poly(A) RNA from polyribosomes of cells pulsed at 1.5 h p.i. (B) Viral RNA from the nucleus of cells pulsed at 1.5 h p.i. (C) Viral poly(A) RNA from polyribosomes of cells pulsed at 5.25 h p.i. (D) Viral RNA from the nucleus of cells pulsed at 5.25 h p.i. The size range of the RNA was determined from the migration of ^{32}P-labeled 28S and 18S rRNA included as an internal size standard. The solid line represents ^{3}H counts per minute; the dotted line represents ^{32}P counts per minute. (E) Poly(A) RNA from polyribosomes of cells pulsed at 1.5 h p.i. was first run on a methylmercury-agarose gel, and then each slice was hybridized in solution to an excess of HSV-1 DNA. The trichloroacetic acid-precipitable ^{3}H counts per minute for each hybridized slice remaining after RNase digestion is shown. The positions of 28S and 18S rRNA's are indicated by arrows. Migration was from left to right. The top scale shows the migration expected for RNA of the size shown in kb.*

Mapping of specific-sized 2 h p.i. HSV-1 mRNA. We have used size-fractionated polyribosomal poly(A) RNA isolated 2 h p.i. for hybridization to Southern blots of restriction fragments of HSV-1 DNA to localize individual viral mRNA species abundant at this time. A typical size distribution of such RNA labeled from 0 to 2 h p.i. and fractionated by electrophoresis on a denaturing gel is shown in Fig. 2. We found that the two peaks of radioactivity shown by the arrows in Fig. 2 migrated with sizes of 4.1 kb and 1.8 kb, respectively. This was determined by fractionating ^{3}H-labeled polyribosomal poly(A) RNA, labeled from 0 to 2 h p.i., with ^{32}P-labeled rRNA markers. In the gels used for blot hybridization, a parallel gel of ^{32}P-labeled rRNA was run to confirm our size assignments.

After electrophoresis, gels were sliced into 3-mm slices, and individual slices were hybridized to HSV-1 DNA restriction fragment blots. As shown in Fig. 3, the restriction endonucleases *Hin*dIII, *Xba*I, *Bgl*II, and *Hpa*I, used singly or in concert, yielded restriction fragments which could be easily separated and which represented the entire HSV-1 genome. Blots of *Hin*dIII digests, *Bgl*II digests, and *Hin*dIII/*Xba*I double

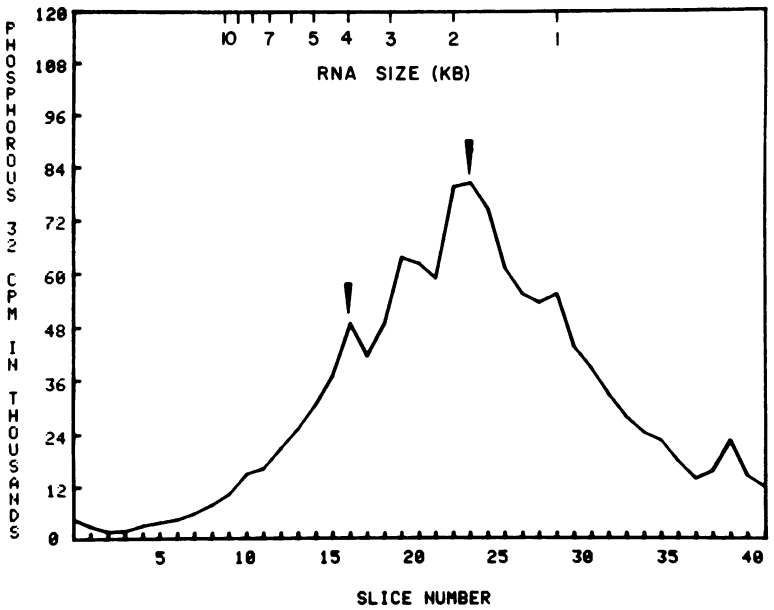

FIG. 2. *Size distribution of polyribosomal poly(A) RNA from HSV-1-infected cells. In the experiment shown, the polyribosome-associated poly(A) RNA from 8 × 10⁷ cells labeled from 0 to 2 h p.i. with $^{32}P_i$ (500 μCi/ml) was fractionated on a methylmercury-agarose gel. The gel was sliced at 3-mm intervals, and the radioactivity was determined for each slice by counting Cerenkov radiation. The size range of the RNA was determined from the migration of 28S and 18S rRNA in a parallel gel, as well as from the positions of the 4.1-kb and 1.8-kb RNA species marked by arrows (see text).*

digests were routinely used. Figure 4 shows an autoradiograph of hybrids of size-fractionated RNA to *Hin*dIII/*Xba*I double-digest blots. It is apparent that for any given restriction fragment, hybridization markedly above background was limited to specific sizes of RNA. For example, *Xba*I fragment G hybridized strongly to RNA of 2.6 to 2.9 and 1.3 to 1.6 kb in length. *Hin*dIII fragment IO was seen to hybridize well to species 4.3 and 2.5 kb in size. Similarly, the hybridization of discrete RNA sizes was concentrated in specific restriction fragments. As can be seen, the 5-kb RNA only hybridized to *Hin*dIII fragment K. A more complex pattern of hybridization, although still highly specific, was seen for most of the RNA sizes. The most complex case was with RNA migrating from 1.7 to 1.9 kb in size. This hybridized to the half molar fragments *Hin*dIII D and *Hin*dIII G, as well as to the quarter molar fragments *Hin*dIII B, *Hin*dIII C, *Hin*dIII E, and *Hin*dIII F and the molar fragment *Hin*dIII N. Further, this size of RNA hybridized to *Hin*dIII fragment M and the partial fragment of *Hin*dIII L (LE), which run together in double-digest blots. In *Hin*dIII digest blots, it was seen that both *Hin*dIII fragments L and M showed hybridization. As discussed further below, such complex patterns of hybridization are due both to having RNA of similar sizes from different regions of the genome and to the fact that different submolar restriction fragments can contain the same DNA sequence (Fig. 3).

The results of hybridization to *Hin*dIII/*Xba*I double-digest blots, along with the data from blots of *Bgl*II and *Hin*dIII digests, are summarized in Table 1. The basis for assignment of specific-sized RNA to a given restriction fragment is as described below. The sizes shown are the result of comparing the three types of blots and are within ±10% of the exact value for any given RNA size. Often, a specific RNA size species was seen to hybridize to separated regions of the HSV-1 genome, suggesting that more than one RNA species of that size was present. This was shown to be the case by 3′ end analysis of the RNA species in question (see below). For example, RNA of 3.8 to 4.2 kb hybridized to submolar *Hin*dIII fragments containing the short repeat region (S_R) as predicted from the hybridization to *Hin*dIII fragments G and M. Less intense, but significant, hybridization was seen to *Hin*dIII fragment IO. Another intense area of hybridization was seen in the band containing *Xba*I fragment F and *Hin*dIII fragment E. The majority of radioactivity in this band must be due to fragment *Xba*I F, since hybridization to *Hin*dIII fragment E should be no more intense than to *Hin*dIII fragment B or C. This,

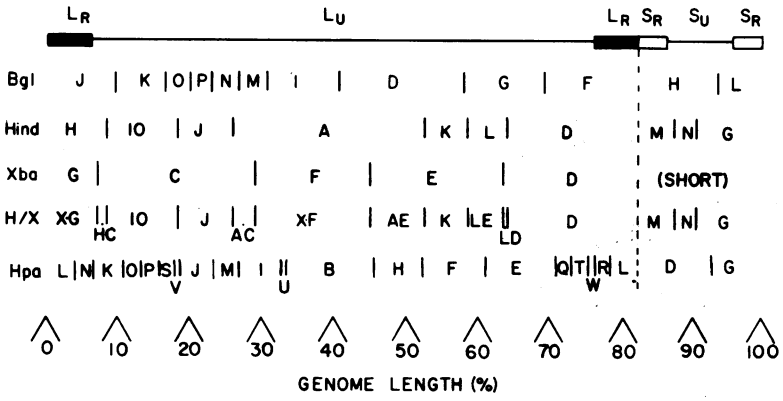

FIG. 3. *Map of restriction endonuclease fragments of the KOS strain of HSV-1. The fragments generated by cleavage by the restriction endonuclease BglII, HindIII, XbaI, HpaI, and HindIII/XbaI double digests are shown for the prototypical arrangement (P) of our HSV-1 strain (1). The solid boxes at the ends of the long segment represent the L_R sequences; the open boxes on the short segment represent the S_R sequences. Three other arrangements occur (12, 40). These are I_L, where the long segment is inverted relative to the short; I_S, where the short segment is inverted relative to the long; and I_{LS}, where both the long and short segments are inverted relative to the prototype. These arrangements have no effect on the yield of fragments which are totally contained by cleavage sites in either the long or the short segment, but do lead to submolar bands for fragments coming from the ends of molecules and those bridging the junction between the long and short segments. Submolar fragments for the endonucleases shown are as follows: half molar fragments arise from ends of molecules; BglII L, HindIII G, and HpaI G are from P and I_L. BglII J, HindIII H, XbaI A (XbaI D+ short region), and XbaI G are from P and I_S. BglII F, HindIII D, XbaI B (XbaI G+ short region), and XbaI D are from I_L and I_{LS}. BglII H, HindIII M, and HpaI D are from I_S and I_{LS}. The terminal HpaI fragment L is generated by a site within the long repeat; thus, it occurs as a molar fragment, containing only L_R sequences. Quarter molar fragments arise as the sum of the half molar fragments from either side of the junction for each arrangement: BglII A is F + H, and HindIII C is D + M. These regions are contiguous in P. BglII B is J + H, and HindIII F is H + M. These regions are contiguous in I_L. BglII C is F + L, and HindIII B is D + G. These regions are contiguous in I_S. BglII E is J + L, and HindIII E is H + G. These regions are contiguous in I_{LS}. XbaI has no cleavage sites in the short segment; therefore, the half molar fragments XbaI A and XbaI B have both arrangements of the short region. Since HpaI has a site within the L_R, no quarter molar fragments occur. Thus, HpaI A (L + D) arises from P and I_L, and HpaI C (L + G) arises from I_S and I_{LS}. Double-digest fragments are designated as follows. HindIII fragments unaltered by the additional digestion with XbaI are shown with the same designation as for HindIII digestion alone. XbaI fragments unaltered by the additional digestion with HindIII are shown with an "X" preceding the same designations as for the fragment generated by XbaI digestion alone. New fragments generated by double digestion are indicated by a double letter. This designation represents the corresponding fragment of the HindIII and XbaI single digest. Fragment HC represents the sequence shared by HindIII fragment H and XbaI fragment C, fragment AC represents overlap between HindIII A and XbaI C, fragment AE represents overlap between HindIII A and XbaI E, fragment LE represents overlap between HindIII L and XbaI E, and fragment LD represents overlap between HindIII L and XbaI D. HindIII fragment IO is a result of the absence of a restriction site in our strain of HSV-1 (29).*

plus evidence showing hybridization to *Bgl*II fragment I, indicates to us the presence of three transcripts of nearly the same size, one near the center of the long unique region (L_U), one near the left end of L_U, and the other located at least in part within S_R. The two transcripts in L_U are measurably larger than the one in S_R since hybridization to *Xba*I fragment F and *Hin*dIII fragment IO was readily detectable in the preceding slice, which showed little hybridization to *Hin*dIII fragments G and M. RNA 2.8 kb in size hybridized well to *Hin*dIII fragments G and N, but not to M. It also hybridized to *Bgl*II bands L and G-H and the submolar bands containing the long repeat (L_R) sequences. This indicates three transcripts of 2.8 kb, two of which come from the short unique (S_U) region. One of these is located in *Hin*dIII fragment N, possibly overlapping into *Hin*dIII fragment G, whereas the other is in *Bgl*II fragment L, possibly extending into *Bgl*II fragment H, but not into S_R. The third 2.8-kb mRNA comes from L_R. Other examples of putative multiple species of HSV-1 mRNA of the same size are shown in Table 1.

It is apparent as shown in Fig. 4 that different amounts of hybridization occurred for different RNA species. This indicates that variable amounts of specific viral mRNA's were synthesized, or at least were present on polyribosomes, during the label time. The spot representing the

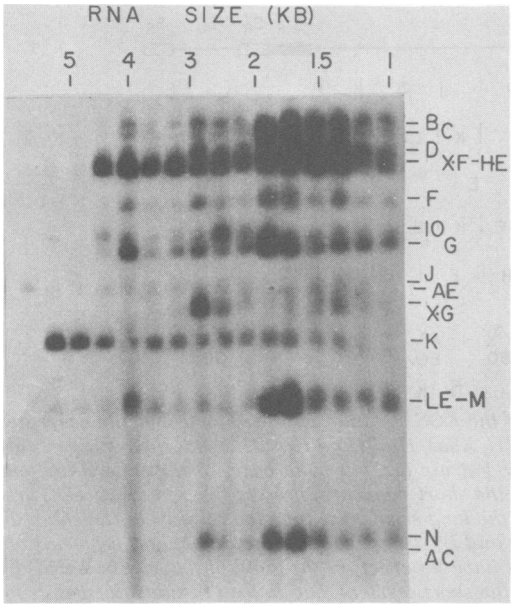

FIG. 4. *Hybridization of size-fractionated HSV-1 mRNA to DNA restriction fragment blots. Individual slices of the ^{32}P-labeled RNA fractionated in Fig. 2 were dissolved in hybridization buffer containing 65% formamide and hybridized to strips of Southern blots of HSV-1 DNA, which had been digested with both HindIII and XbaI endonucleases. The locations of these cleavage sites and the orientation of the resulting fragments are shown in Fig. 3. After hybridization at 55°C for 24 h, strips were rinsed and arranged according to the size of RNA used. These were then autoradiographed for 20 h at −70°C, using two intensifying screens.*

2.5-kb transcript from *Hin*dIII fragment IO is much more intense than the 4.2-kb *Hin*dIII fragment IO transcript. Both of these are less intense than the 2.8-kb transcript hybridizing to *Xba*I fragment G. In addition to those shown in Table 1, other RNA species labeled from 0 to 2 h p.i. hybridized to a smaller, but still detectable, extent with restriction fragments. Thus, there was detectable RNA of various sizes hybridizing to *Hin*dIII fragment J. Other such examples occurred throughout the HSV-1 genome, and we have only included those RNA species in Table 1 which were reproducibly present in readily detectable quantities in several experiments.

In contrast to the well-resolved HSV RNA sizes hybridizing to most restriction fragments, variable amounts of RNA ranging from less than 3 to 5 kb hybridized to *Hin*dIII fragment K, in addition to the RNA 5.1 to 5.3 kb in size. This phenomenon is also seen with later labeling times, although in those cases, specific sizes predominate (1). The reason for this is unclear; however, as will be discussed below, all RNA hybridizing to this fragment has a 3′ end mapping in the same location. In Table 1, we have only indicated the largest HSV mRNA species hybridizing to *Hin*dIII fragment K.

Localization of 3′ ends of 2 h p.i. HSV mRNA. The assignment of a given size of HSV-1 mRNA to several locations on the viral genome, as described in Table 1 for certain sizes of RNA, is consistent with either a single mRNA molecule being encoded by distantly placed noncontiguous regions of the genome or several mRNA's of similar sizes being encoded. To estimate the number of discrete 3′ ends for the HSV-1 mRNA of the sizes shown in Table 1, we carried out blot hybridizations of cDNA made to the 3′ ends of various size ranges of HSV-1 polyribosomal poly(A) mRNA present at 2 h p.i. We labeled cells with a small amount of $^{32}P_i$ from 0 to 2 h p.i. and isolated polyribosomal poly(A) RNA. Such RNA was fractionated as described for Fig. 2, and slices of the gel containing radioactive label were pooled into size ranges of 5.0 to 5.8, 4.2 to 4.8, 3.2 to 4.0, 2.3 to 3.0, 1.7 to 2.0, and 1.4 to 1.7 kb. RNA was partially degraded to an average length of 400 to 500 bases (see above), the nicked RNA was eluted from the slices, and poly(A)-containing 3′ ends of this RNA were isolated using oligo(dT)-cellulose. ^{32}P-labeled 3′ cDNA was synthesized using reverse transcriptase as described above. The cDNA made had an average size range of 10 to 100 nucleotides as determined by its migration on denaturing agarose gels (see above).

The 3′ probe cDNA from RNA of different size ranges was hybridized in separate experiments to blots of either *Hin*dIII/*Xba*I double digests, *Hin*dIII, or *Hpa*I digests or HSV-1 DNA. Specific examples of such autoradiographs are shown in Fig. 5A, B, C, E, F, G, and I. Guide strips of comparable blots showing band resolution are also shown (Fig. 5D, H, and J). Data from all experiments are summarized in Table 1. The patterns of hybridization of the 3′ probe cDNA for each size range were entirely consistent with the RNA species that we identified in Fig. 4. In most cases, the 3′ ends of the molecules mapped in the same restriction fragments as the bulk of the mRNA, and interpretation of the data is routine. In several cases, however, multiple species of mRNA of similar sizes gave a more complex pattern. Further, in three instances, the localization of the 3′ end of the viral mRNA suggested the direction of transcription of the molecule. These cases are discussed below.

We found that 3′ cDNA of 2 h p.i. HSV-1 mRNA migrating at a size of 5 to 5.8 kb mapped in *Hin*dIII fragment L (Fig. 5E). Since HSV-1

TABLE 1. *Location of abundant early HSV-1 mRNA*[a]

Size of RNA (kb)[b]	Major restriction fragment bands hybridizing to RNA[c]	Restriction fragment band hybridizing to 3′ end probe of 2 h p.i. RNA of size range indicated[c]		Location of mRNA on HSV-1 genome segment[d]	Fractional genome length (%)[e]	Presence of RNA of similar size at 39°C after infection with *ts*B2
5.3	H(K); B(D-E)	H(L)	5–5.8 kb	L_U	53–60	(+)[f]
4.3	X(F)-H(E); B(I); B(D-E)	X(F)-H(E)	4.2–4.8 kb	L_U	31–45	–
4.2	H(IO)	H(IO)		L_U	9–18	–
4	H(G); H(M); B(L)	H(G)	3.2–4 kb	S_U-S_R	91–100	–
3.3	X(F)-H(E)	X(F)-H(E)		L_U	31–45	–
2.8	X(G); H(D); B(F); B(J)	H(H)[g]	2.3–3 kb	L_R	0–6	+
	H(N)	H(N)		S_U	86–96	–
	H(G)	H(G)		S_U	86–96	?
2.5	H(IO); B(O); B(K)	H(IO)		L_U	10–18	–
1.8	H(G)	H(A-B-C); X(F)-H(E); H(G)	1.7–2 kb	S_U	91–96	+
	H(D)	H(D-E); Hpa(S-T)		L_U	65–76	+
	H(N); H(M)	H(N)		S_R-S_U	82–91	+
	H(L)	H(L)		L_U	59–65	?
1.5	X(F)-H(E); B(I); B(M)	H(A-B-C); X(F)-H(E)	1.4–1.7 kb	L_U	29–41	–
	X(G); B(J); H(H)	H(H); H(D-E); H(F)		L_R	0–6	–
	H(G); B(G-H)	H(G)		S_U	91–96	–

[a] Summary of data from Fig. 4, 5, and 7, as well as blot hybridizations not shown.
[b] The sizes shown represent the best estimate, as determined from several experiments, and are within ± 10%.
[c] B indicates a band derived from *Bgl*II digestion, H is from a *Hin*dIII digest, X is from an *Xba*I digest, and Hpa is from an *Hpa*I digest.
[d] See Fig. 3.
[e] As measured from the left end of the P arrangement.
[f] RNA hybridizing to this region is seen at the nonpermissive temperature, but as a smaller size than that found in a wild-type infection (see text).
[g] Seen at 39°C after infection with *ts*B2.

RNA 5.3 kb in size and smaller hybridized to *Hin*dIII fragment K (Fig. 4), this suggested that its 3′ end is on the *Hin*dIII fragment L side of the junction of these two fragments in the HSV-1 genome. This tentative conclusion has been confirmed by using purified 5.2-kb mRNA for probe template (K. P. Anderson, L. E. Holland, B. H. Gaylord, and E. K. Wagner, manuscript in preparation). Pools of smaller RNA also yielded 3′ probe hybridizing to *Hin*dIII fragment L, or the band containing double-digest fragment LE, in keeping with the finding of RNA between 3 and 5 kb in size hybridizing to *Hin*dIII fragment K (Fig. 5A, B, and C).

RNA 3.2 to 4 kb in size gave 3′ probe cDNA hybridizing to *Xba*I fragment F (Fig. 5B). This 3′ end corresponds to the 3.3-kb RNA found hybridizing to this region. There also was hybridization of the 3′ probe to *Hin*dIII fragment G and to the band containing double-digest fragment LE and *Hin*dIII fragment M. Since no hybridization to *Hin*dIII fragment M was detected in other blots using this same 3′ probe (data not shown), the 3′ end of this mRNA species was localized to the S_U region of *Hin*dIII fragment G. This 3′ probe is then consistent with its belonging to the 4-kb mRNA species of Fig. 4 hybridizing to *Hin*dIII fragment G, as well as to the other fragments containing the S_R region. Such results allow us to tentatively conclude that this 4-kb RNA has its 5′ end in the S_R region of *Hin*dIII fragment G and the 3′ end in S_U sequences of that fragment.

The situation with HSV-1 mRNA smaller than 2 kb is complex; we can identify at least seven species in this size range. Of these, four can be identified in RNA of 1.7 to 2.0 kb; RNA of this size yields 3′ cDNA hybridizing to *Hin*dIII fragments (A,B), C, (D,E), F, G, L, and N (Fig. 5F). In *Hin*dIII/*Xba*I double digests, hybridization was similarly complex. Radioactivity was seen in *Hin*dIII bands B, C, and G, and the

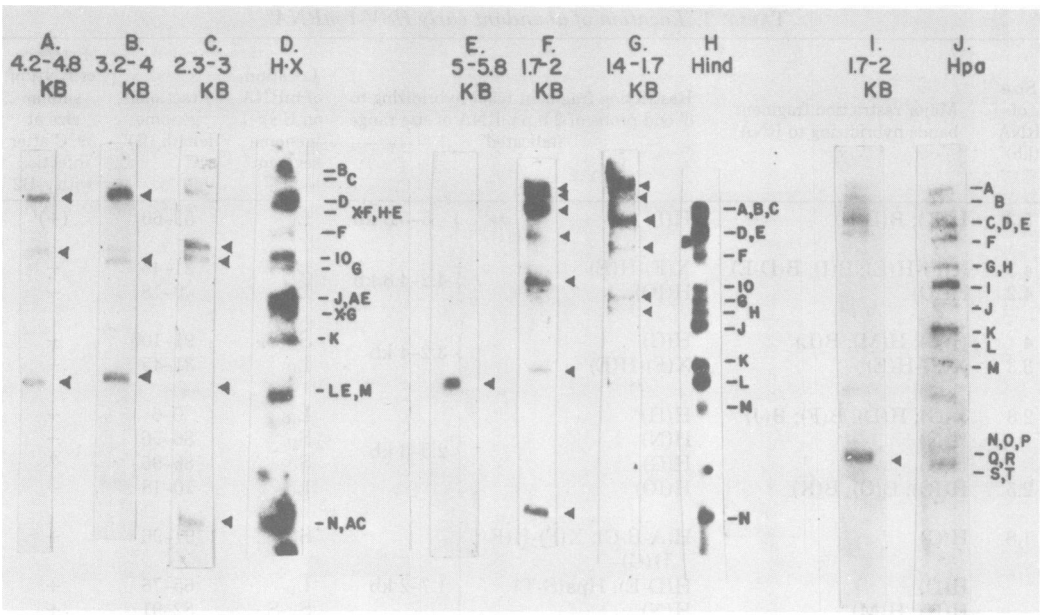

FIG. 5. *Hybridization of 3′ probe cDNA to DNA restriction fragment blots. ^{32}P-labeled DNA probe complementary to the 3′ ends of size-fractionated mRNA was made using reverse transcriptase (see text). This cDNA was then hybridized to Southern blots of restricted HSV-1 DNA at 45°C for 48 h. The strips were rinsed and autoradiographed as in Fig. 4. Panels A to D are hybrids to blots of HindIII/XbaI double digests. Hybridization was with the following. (A) 3′ cDNA made to 2 h p.i. RNA ranging from 4.2 to 4.8 kb in size. The bands showing significant radioactivity are X(F)-H(E), H(IO), and (H/X)LE-(H)M. (B) 3′ cDNA made to RNA from 3.2 to 4 kb in size. Radioactivity is in bands X(F)-H(E), H(G), and (H/X)LE-(H)M. (C) 3′ cDNA made to RNA from 2.3 to 3 kb in size. Radioactivity is in bands H(IO), H(G), (H/X)LE-H(M), and H(N)-(H/X)AC. (D) ^{32}P-labeled HSV-1 DNA used to hybridize to all bands to indicate resolution. Panels E to H are HindIII digest blots. Hybridization was with the following. (E) 3′ cDNA made to 2 h p.i. RNA 5.2 to 5.8 kb in size. Radioactivity is to band H(L). (F) 3′ cDNA made to RNA 1.7 to 2 kb in size. Radioactivity is in bands A-B, C, D-E, F, G, L, and N. (G) 3′ cDNA made to RNA 1.4 to 1.7 kb in size. Radioactivity is in bands A-B, C, D-E, F, G, and H. (H) ^{32}P-labeled HSV-1 DNA, sonicated to produce small fragments, was used to hybridize to all bands to indicate resolution. Panels I and J are HpaI blots. Hybridization was with the following. (I) 3′ cDNA made to 2 h p.i. RNA 1.4 to 1.7 kb in size. Major radioactivity is in band S-T. (J) A pooled mix of 2 and 6 h p.i. ^{32}P-labeled RNA was used to hybridize all bands to indicate resolution. The faint band of radioactivity above the band containing HpaI fragments P, Q, and R is a partial-digest fragment that is occasionally seen.*

mixed band of *Xba*I (F)-*Hin*dIII (E), as well as in some other bands. There was, however, no significant hybridization to *Hin*dIII fragment M and *Xba*I fragment G, so no 3′ end of HSV-1 RNA of 1.7 to 2 kb maps in either the L_R or S_R region. The data are consistent with two species of RNA 1.7 to 2 kb in size mapping in S_U, one with its 3′ end in the unique part of *Hin*dIII fragment N and the other in the unique region of fragment G. The latter is marginally larger than the former by virtue of the greater intensity of hybridization to *Hin*dIII fragment G one slice earlier than to fragment N (Fig. 4). The smaller mRNA species, which has its 3′ end in *Hin*dIII fragment N, must have its 5′ end in *Hin*dIII fragment M, since RNA of this size hybridizes to this area and no 3′ end is found in fragment M.

A third species of approximately 1.8 kb in size can be mapped in the long region of the HSV-1 genome found in *Hin*dIII fragments B, C, and D. We took the cDNA after hybridization to the double-digest blot and hybridized it to a blot of an *Hpa*I digest of HSV-1 DNA. Hybridization was seen in the band containing fragments S and T. From this we can map this third 1.7- to 2-kb HSV-1 mRNA to the L_U regions of the HSV-1 genome between 65 and 76% from the left end of the prototypical (P) arrangement. This correlates with the finding of HSV mRNA of this size from the blot hybridization of total RNA shown in Fig. 4. Finally, a fourth species can be mapped in the L_U region bounded by *Hin*dIII fragment L since there is an HSV-1 mRNA species 1.8 kb in size that hybridizes to that region.

Pooled RNA of 1.4 to 1.7 kb in size gave 3′

probe which hybridized best to *Hin*dIII fragments (A,B), C, (D,E), F, G, and H (Fig. 5G). Blots of double digests of *Hin*dIII/*Xba*I showed the cDNA hybridizing to the mixed band *Xba*I (F)-*Hin*dIII (E). These data suggest that three mRNA species of this size are abundant at 2 h p.i. Since RNA of this size was seen to hybridize to *Xba*I fragment G (Fig. 4), one of these mRNA species has been mapped in L_R. A second mRNA species of this size is located in the S_U region of *Hin*dIII fragment G. The data are consistent with a third being in the center of the L_U region, which was indicated by hybridization of RNA of this size to *Bgl*II fragments I and M (Table 1).

Characterization of HSV-1 mRNA in a DNA-negative *ts* mutant. We used the methods outlined in the previous sections to investigate the properties of HSV-1 mRNA synthesized after infection with the mutant *ts*B2. We examined the size distribution of the viral mRNA synthesized under nonpermissive conditions as follows. A culture of 8×10^7 cells, infected with a multiplicity of 7 PFU of *ts*B2 virus per cell, was labeled at 39°C with $^{32}P_i$ from 2 to 9 h p.i. Polyribosomal poly(A) RNA was prepared, and viral RNA was isolated by hybridization to HSV DNA cellulose. The RNA was fractionated on a denaturing agarose gel, and as shown in Fig. 6, the viral mRNA migrated as three major bands. The sizes of these bands were estimated to be 4, 3, and 1.9 kb, based on the position of HeLa cell rRNA run in a parallel gel. In a parallel experiment, cells infected with *ts*B2 were incubated at the permissive temperature (34°C) for the same period of time. The size distribution of polyribosomal viral RNA in this case was essentially the same as that seen late after infection.

At the nonpermissive temperature, a small amount of material migrating in the range of 5.2 to 6.5 kb was seen, as well as in the three major bands. The bands of radioactivity were pooled as shown in Fig. 6 with RNA ranging in the pools as follows: pool 1, 5 to 6.5 kb; pool 2, 3.8 to 4.5 kb; pool 3, 2.2 to 3.5 kb; pool 4, 1.7 to 2 kb; and pool 5, 1.3 to 1.6 kb. We used this RNA as a template to make 3′ cDNA probe, and this material was hybridized to blots of *Hin*dIII restriction fragments of HSV-1 DNA.

Autoradiographs of the hybridized cDNA probe are shown in Fig. 7. No hybridization was seen with pool 1 or pool 5 3′ probe. Pool 2, 3′ probe hybridized only to *Hin*dIII fragment L (Fig. 7A), and radioactivity hybridizing to this band was seen in pools 3 and 4 also. This type of broad migration was seen with the HSV-1 mRNA hybridizing to *Hin*dIII fragment K in infections with wild-type virus. With infection at 39°C, however, no significant amounts of this

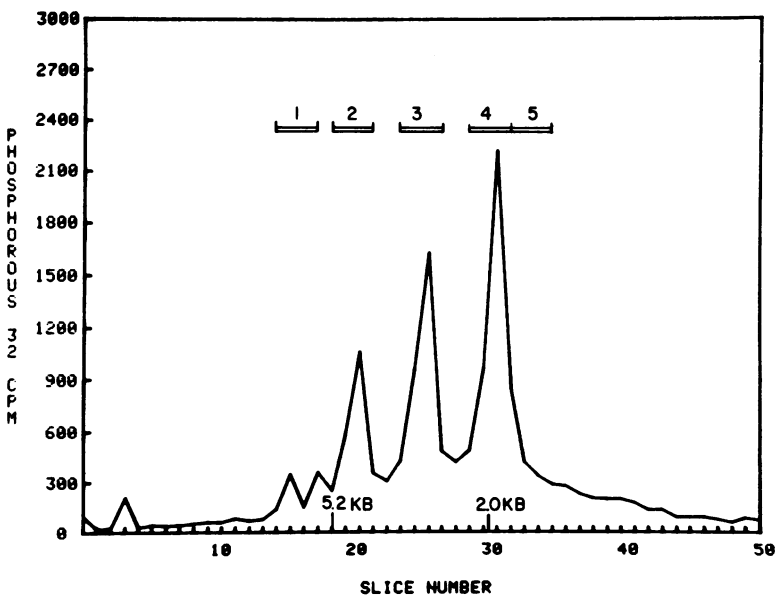

FIG. 6. *Size distribution of HSV-1 mRNA present at 39°C after infection with the DNA-negative mutant tsB2. Cells (8×10^7) were infected for 1 h at 37°C with the mutant virus and then incubated at 39°C. Beginning at 2 h p.i., the cells were labeled for 7 h with $^{32}P_i$ (80 μCi/ml). The polyribosome-associated poly(A) RNA was isolated and hybridized to HSV-1 DNA cellulose (see text). The viral RNA was gel fractionated and counted as described in the legend to Fig. 2. The location of 5.2- and 2.0-kb RNA was determined from rRNA migration in a parallel gel. Bars indicate the regions pooled for 3′ end analysis (see text).*

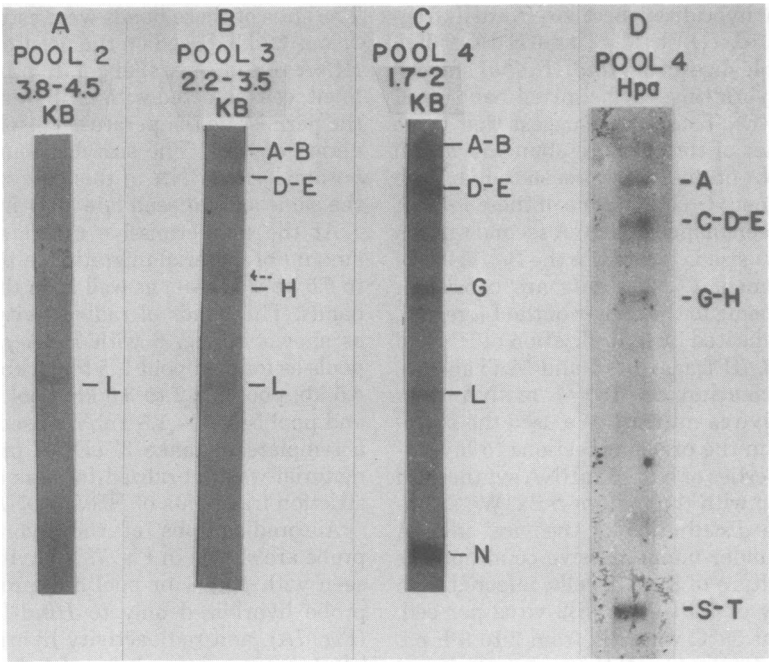

FIG. 7. *Hybridization of 3' probe cDNA prepared from RNA produced by tsB2 at the nonpermissive temperature. (A) cDNA made from 3.8- to 4.5-kb RNA (Fig. 6, pool 2) hybridized to a blot of HindIII-digested HSV-1 DNA. (B) cDNA made from 2.2- to 3.5-kb RNA (Fig. 6, pool 3) hybridized to a HindIII digest blot. The dashed line indicates a slight amount of radioactivity in band H(G). (C) cDNA made from 1.7- to 2.0-kb RNA (Fig. 6, pool 4) hybridized to a HindIII digest blot. (D) The cDNA of (C) was rehybridized to an HpaI blot. Resolution of bands is comparable to those shown in Fig. 5. Autoradiography was for 2 weeks without screens.*

RNA larger than 4.3 kb were seen. It is possible that this RNA is uniquely susceptible to degradation, accounting for these findings.

Pool 3, 3' probe hybridized to *Hin*dIII fragments (A-B), (D-E), H, and L (Fig. 7B). This is consistent with the band of RNA migrating around 3 kb being from the same region as the mRNA from the L_R region found migrating at 2.8 kb in the wild-type infection. A small amount of hybridization also was seen to *Hin*dIII band G, and we suggest that another RNA species similar to the 2.8-kb species mapping in the S_U region with wild type may be present.

The 3' probe cDNA from the RNA pool ranging in size from 1.7 to 2 kb hybridized to *Hin*dIII fragments (A-B), (D-E), G, L, and N (Fig. 7C). Further, the material hybridized to the *Hpa*I band containing fragments S and T in a second hybridization (Fig. 7D). These results are consistent with this band containing three mRNA species, one in the L_U region of *Hin*dIII fragments B and D and two with 3' ends in the S_U region. Because the broadly migrating RNA from *Hin*dIII fragment K has its 3' end in *Hin*dIII fragment L, we cannot establish whether the 1.8-kb mRNA species hybridizing to *Hin*dIII fragment L is present at 39°C. At the highest levels of resolution, low amounts of hybridization can be detected to regions other than just described. The five species discussed, however, represent the most abundant ones present at 39°C after infection with the *ts*B2 mutant.

DISCUSSION

Size distribution of HSV-1 mRNA present in the absence of viral DNA synthesis. The size distribution of 2 h p.i. HSV-1 mRNA is complex, as shown in Fig. 1A, with RNA migrating between 1.5 and 5 kb being isolable in good yield. On the basis of size distribution, this 2 h p.i. viral mRNA is a subset of the viral mRNA present at 6 h p.i. or at other times when viral DNA replication is proceeding at a high rate. Further, the viral mRNA synthesized at 39°C after infection of cells with the *ts*B2 mutant corresponds by size analysis to species of viral RNA seen at 2 h after infection with wild-type virus.

At 2 h p.i., the size distribution of viral RNA in the nucleus was similar to that seen on polyribosomes (Fig. 1A and B). This suggests that nuclear precursors of the polyribosomal poly(A) viral mRNA are essentially the same size as the mRNA and is consistent with the promotors for

the 2 h p.i. mRNA species being near the coding sequences for this mRNA. This is in marked contrast to the situation at 6 h p.i. and later times when nuclear viral RNA labeled in the pulse time had a significantly larger average size than that on polyribosomes.

Localization of abundant 2 h p.i. HSV-1 mRNA on the viral genome. By hybridizing size-fractionated polyribosomal poly(A) RNA, we have been able to map 16 readily identifiable viral mRNA species present at 2 h p.i. This map is shown in Fig. 8. Each of the viral mRNA species shown in this map can be correlated with a 3′ end either within or adjacent to the restriction fragment to which it hybridizes (Table 1). In many instances, a specific size class of mRNA hybridized to noncontiguous regions of the genome (Fig. 4), and 3′ cDNA probe made to that size class also hybridized to the same specific, noncontiguous regions (Fig. 5). The simplest explanation is that each such region codes for a different distinct mRNA species of that size. However, we cannot completely rule out the possibility of some complex pattern of splicing occurring very near the 3′ end of a single mRNA.

The number of mRNA species identified here must be taken as a minimum estimate, as it is not possible to distinguish between single and multiple mRNA species of nearly the same size being encoded within the same restriction fragment. For example, a large restriction fragment could encode several mRNA species of similar size in their entirety, which would appear as only one species in our analysis. The genetic complexity of the mRNA species listed in Table 1 and shown in Fig. 8 represents 32% of the single-strand equivalent coding capacity for HSV-1. At 2 h p.i., abundant HSV-1 mRNA is encoded by nearly half of the single-strand equivalent coding capacity of the viral genome (16, 31, 33). Although the 16 early mRNA species described here account for a substantial portion of the established sequence complexity for abundant early mRNA, it is clear that additional species must be present. Characterization of additional restriction enzyme maps should prove useful in their identification.

On the map shown in Fig. 8, we have localized each transcript to as small a region as possible by using the data derived from hybridization of size-fractionated RNA to blots (Table 1). The uncertainty range is indicated by the brackets. RNA species mapped to the L_R region are shown in both of the possible locations; however, in these experiments we were unable to determine whether these transcripts arise equally from both locations.

In three cases, we have indicated a direction of transcription for the viral mRNA by virtue of the position of the 3′ end of pooled RNA of the size range of interest. Thus, the 3′ end of the 4-kb mRNA mapping in the S_R region has been assigned to the unique region of *Hin*dIII fragment G. The 1.8-kb mRNA species hybridizing to *Hin*dIII fragments M and N has been shown with a 3′ end in fragment N, and thus its 5′ end

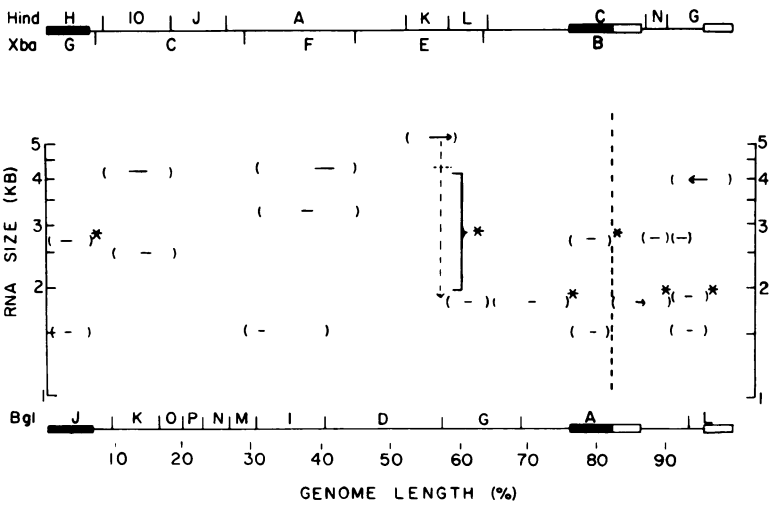

FIG. 8. *Position map of abundant HSV-1 mRNA species present before DNA synthesis. The data of Table 1 and Fig. 4, 5, and 7 on the localization of the mRNA species are summarized and shown here. The locations of the HindIII, XbaI, and BglII restriction fragments are shown for the P orientation, along with the percentage length from the left end of the genome. The RNA size is indicated by both its relative vertical position and the length of the line. The positional limits for each mRNA are indicated by brackets. RNA species denoted with asterisks were present at 39°C in the tsB2 mutant.*

in M. Because of the other slightly larger mRNA species hybridizing to *Hin*dIII fragment G, we were unable to determine whether the 5′ end is located within the S_R or S_U region of *Hin*dIII fragment M. Also, the RNA hybridizing to *Hin*dIII fragment K has been shown with its 3′ end in *Hin*dIII fragment L. We have also indicated the broad size distribution less than 5.3 kb of HSV-1 mRNA hybridizing to *Hin*dIII fragment K with a dashed line in Fig. 8.

Only a limited number of mRNA species are present on polyribosomes at 39°C in cells infected with the *ts*B2 mutant. As indicated in Table 1, the sizes of 5 of the 16 2 h p.i. RNA species are similar to those seen in the mutant by mapping 3′ ends. We have identified the viral RNA species made at 39°C with the *ts* mutant with asterisks in Fig. 8. RNA hybridizing to *Hin*dIII fragment K has been inferred to be present at 39°C because of the presence of 3′ cDNA hybridizing to *Hin*dIII fragment L being synthesized from sizes of RNA between 4.3 and 1.7 kb. It is clear from the size distribution of total HSV-1 mRNA made at 39°C, however, that the 5.3-kb mRNA species, which is normally the predominant one hybridizing to *Hin*dIII fragment K, is not present. We have indicated the smaller size of the RNA transcribed from this region at 39°C with *ts*B2 in Fig. 8 by bracketing the size ranges seen.

The correlation between R-loop mapping (29) and the location of total early transcripts determined here is fairly good. Six of the transcripts identified are located in the short region, in keeping with the large amount of R-looping in this area. The region near the center of the L_U segment contained in *Hin*dIII/*Xba*I double-digest fragment AE does not hybridize efficiently with any discrete mRNA species identified, which is consistent with the absence of large amounts of 2 h p.i. mRNA being encoded by this region as determined by the other methods. Other regions of the long segment of the HSV-1 genome are homologous to limited numbers of specific viral mRNA species.

When the map of the 2 h p.i. mRNA molecules identified in this report is compared with the map for at least twice this number of mRNA species seen at 6 h p.i. reported elsewhere (1), it is clear that RNA the same size as the 2 h p.i. species is still synthesized at 6 h p.i. At 6 h p.i., 2.8-kb mRNA hybridized poorly to blots containing the L_R region of the HSV-1 genome, suggesting that it is present in low abundance at this time after infection. However, its presence could be readily detected in mRNA labeled with a 45-min pulse of [^{3}H]uridine and isolated by DNA cellulose hybridization. The 4-kb mRNA species seen in the short region defined by *Hin*dIII fragment G is also present late at amounts lower than those seen here. These two mRNA species are the sizes that we have identified which are lower in abundance after HSV DNA replication than before.

In addition to mRNA species similar in size to those seen here, a number of other mRNA species became abundant concomitant with viral DNA replication. Some of these appear in regions where 2 h p.i. RNA is rare, such as in the center of the L_U region encompassed by *Hin*dIII/*Xba*I double-digest fragment AE and in *Hin*dIII fragment J. In *Hin*dIII region K, a new species of RNA 7.4 kb in size is seen at 6 h p.i. Further, at the later time, a species of mRNA 3.8 kb in size becomes clearly defined, whereas at 2 h p.i., RNA of this size hybridizing to *Hin*dIII fragment K is only seen within the broad size distribution of RNA less than 5 kb. Although significant synthesis of HSV-1 mRNA larger than 5 kb is the most striking new feature of 6 h p.i. RNA synthesis compared with that described here, additional mRNA's of all size ranges are seen. Together, these could account for the increase from 2 to 6 h p.i. of 20–25% to 45% of HSV-1 DNA being saturated by abundant RNA.

Correlation between the viral mRNA species present in the absence of viral DNA synthesis and early viral proteins. Use of intertypic recombinants between HSV-1 and HSV-2 has led to the localization of 10 to 13 virus-specific α and β polypeptides (19, 23). The largest of the polypeptides identified is ICP-4 with a size of 170,000 d, which has been mapped in the *Hin*dIII G end of the short region of the HSV-1 genome. Such a polypeptide is within the coding capacity of the 4-kb mRNA identified here as being encoded by this region of the genome. Another large polypeptide, ICP-7, which is 150,000 d in size, maps at 55 to 65% from the left end of the long segment in the P arrangement, and this correlates well with the 5-kb mRNA species that we have mapped in *Hin*dIII fragment K. The determinant for phosphonoacetic acid sensitivity has been shown to reside in the structural gene for the 149,000-d, HSV-1-specified DNA polymerase (24). The 4.3-kb mRNA mapping at 31 to 45% in the L_U region is of sufficient size to code for the polymerase and compares favorably with the position mapped for phosphonoacetic acid resistance. Also, the viral deoxypyrimidine kinase has been localized at about 30% in L_U (19), correlating nicely with one of the small mRNA's that we have identified. In summary, of the α and β polypeptides presently localized, nine correlate

very well in both size and location with mRNA's that we have mapped. It is interesting, however, that as has been seen with HSV-1 mRNA species present at 6 h p.i., the smallest HSV-1 mRNA species seen at 2 h p.i. (1.5 kb) have significantly more coding capacity than required to encode the smallest polypeptides (32,000 d [19]) and, thus may contain significant untranslated RNA.

In the correlation between mRNA and proteins seen at 39°C with the *ts*B2 mutant, the situation is somewhat less clear. Courtney et al. (7) have reported that five polypeptides ranging in size from 175,000 to 24,000 d are produced in large amounts at 39°C in cells infected with the *ts*B2 mutant. This correlates well with the size and numbers of viral mRNA species seen at 39°C with this mutant. Both Jones et al. (15) and Clements et al. (6) have reported that α or immediate early RNA maps in the locations where we have located the abundant *ts*B2 mRNA species. Our localizations also agree with those reported by Watson and Clements (38) with a similar *ts* mutant (*ts*K) and extend their observations by providing a size for these transcripts. Further, Preston et al. (23) have mapped the location of five immediate early proteins which correlate well in size with the proteins overproduced by *ts*B2. These observations suggest that the mRNA species that we have identified at 39°C are α mRNA species. However, the 170,000-d α protein seen at 30°C with *ts*B2 has been located in the S_R region of the viral genome by both Morse et al. (19) and Preston et al. (23); therefore, the correlation is not absolute since we do not see any mRNA larger than 3 kb in this region with the mutant. Further, it is not at all clear what the significance of the truncated RNA from *Hin*dIII region K is in respect to the phenotype of the mutant. It is possible that extraction and size fractionation of the RNA as carried out here may result in some degradation of large RNA species, which would be exacerbated in the *ts* mutant infection.

In summary, the general correlation between the mRNA species seen, their map positions, and the proteins localized at 2 h p.i. is good. Full correlation between a given mRNA species and the protein that it encodes requires determination of the biological activity of the mRNA. Such determinations, as well as higher-resolution mapping of the mRNA species, will result in the detailed map of HSV-1 gene function required for further study of viral gene regulation.

ACKNOWLEDGMENTS

We thank B. Gaylord and L. Tribble for excellent technical assistance. We are also grateful to C. Shipman, Jr., J. Manning, and K. K. Tewari for many helpful discussions.

This work was supported by Public Health Service grant CA-11861 from the National Cancer Institute. K.P.A. was supported by Public Health Service predoctoral training grant GM07311 from the National Institutes of Health.

LITERATURE CITED

1. **Anderson, K. P., J. R. Stringer, L. E. Holland, and E. K. Wagner.** 1979. Isolation and localization of herpes simplex virus type 1 mRNA. J. Virol. **30**:805–820.
2. **Bachenheimer, S. L., and B. Roizman.** 1972. Ribonucleic acid synthesis in cells infected with herpes simplex virus. J. Virol. **10**:875–879.
3. **Bailey, J. M., and N. Davidson.** 1976. Methylmercury as a reversible denaturing agent for agarose gel electrophoresis. Anal. Biochem. **70**:75–85.
4. **Bartkoski, M., and B. Roizman.** 1976. RNA synthesis in cells infected with herpes simplex virus. XIII. Differences in the methylation patterns of viral RNA during the reproductive cycle. J. Virol. **20**:583–588.
5. **Casey, J., and N. Davidson.** 1977. Rates of formation and thermal stabilities of RNA:DNA and DNA:DNA duplexes at high concentrations of formamide. Nucleic Acids Res. **4**:1539–1552.
6. **Clements, J. B., R. J. Watson, and N. M. Wilkie.** 1977. Temporal regulation of herpes simplex virus type 1 transcription: location of transcripts on the viral genome. Cell **12**:275–285.
7. **Courtney, R. J., P. A. Schaffer, and K. L. Powell.** 1976. Synthesis of virus-specific polypeptides by temperature sensitive mutants of herpes simplex virus type 1. Virology **75**:306–318.
8. **Denhardt, D. T.** 1966. A membrane-filter technique for the detection of complementary DNA. Biochem. Biophys. Res. Commun. **23**:641–646.
9. **Dulbecco, R., and M. Vogt.** 1954. Plaque formation and isolation of pure lines with poliomyelitis viruses. J. Exp. Med. **99**:167–182.
10. **Dunn, A. R., and J. A. Hassell.** 1977. A novel method to map transcripts: evidence for homology between an adenovirus mRNA and discrete multiple regions of the viral genome. Cell **12**:23–36.
11. **Grafstrom, R. H., J. C. Alwine, W. L. Steinhart, C. W. Hill, and R. W. Hyman.** 1975. The terminal repetition of herpes simplex virus DNA. Virology **67**:144–157.
12. **Hayward, G. S., R. J. Jacobs, S. C. Wadsworth, and B. Roizman.** 1975. Anatomy of herpes simplex virus DNA: evidence for four populations of molecules that differ in the relative orientations of their long and short components. Proc. Natl. Acad. Sci. U.S.A. **72**:4243–4247.
13. **Holm, C. A., S. G. Oliver, A. M. Newman, L. E. Holland, C. S. McLaughlin, E. K. Wagner, and R. C. Warner.** 1978. The molecular weight of yeast P1 double-stranded RNA. J. Biol. Chem. **253**:8332–8336.
14. **Honess, R. W., and B. Roizman.** 1974. Regulation of herpesvirus macromolecular synthesis. I. Cascade regulation of the synthesis of three groups of viral proteins. J. Virol. **14**:8–19.
15. **Jones, P. C., G. S. Hayward, and B. Roizman.** 1977. Anatomy of herpes simplex virus DNA. VII. α RNA is homologous to noncontiguous sites in both the L and S components of viral DNA. J. Virol. **21**:268–276.
16. **Kozak, M., and B. Roizman.** 1974. Regulation of herpesvirus macromolecular synthesis: nuclear retention of nontranslated viral RNA sequences. Proc. Natl. Acad. Sci. U.S.A. **71**:4322–4326.
17. **Maitland, N. J., and J. K. McDougall.** 1977. Biochemical transformation of mouse cells by fragments of herpes simplex virus DNA. Cell **11**:233–241.
18. **McMaster, G. K., and G. G. Carmichael.** 1977. Analysis of single- and double-stranded nucleic acids on polyacrylamide and agarose gels by using glyoxal and acri-

dine orange. Proc. Natl. Acad. Sci. U.S.A. **74**:4835–4838.
19. **Morse, L. S., L. Pereira, B. Roizman, and P. A. Schaffer.** 1978. Anatomy of herpes simplex virus (HSV) DNA. X. Mapping of viral genes by analysis of polypeptides and functions specified by HSV-1 × HSV-2 recombinants. J. Virol. **26**:389–410.
20. **Moss, B., A. Gershowitz, J. R. Stringer, L. E Holland, and E. K. Wagner.** 1977. 5'-Terminal and internal methylated nucleosides in herpes simplex virus type 1 mRNA. J. Virol. **23**:234–239.
21. **Noyes, B. E., and G. R. Stark.** 1975. Nucleic acid hybridization using DNA covalently coupled to cellulose. Cell **5**:301–310.
22. **Palmiter, R. D.** 1974. Magnesium precipitation of ribonucleoprotein complexes. Expedient technique for the isolation of undergraded polysomes and messenger ribonucleic acid. Biochemistry **13**:3606–3614.
23. **Preston, V. G., A. J. Davison, H. S. Marsden, M. C. Timbury, J. H. Subak-Sharpe, and N. M. Wilkie.** 1978. Recombinants between herpes simplex virus types 1 and 2: analyses of genome structures and expression of immediate early polypeptides. J. Virol. **28**:499–517.
24. **Purifoy, D. J. M., R. B. Lewis, and K. L. Powell.** 1977. Identification of the herpes simplex virus DNA polymerase gene. Nature (London) **269**:621–623.
25. **Sanger, F., G. M. Air, B. G. Barrell, N. L. Brown, A. R. Coulson, J. C. Fiddes, C. A. Hutchison III, P. M. Slocombe, and M. Smith.** 1977. Nucleotide sequence of bacteriophage ϕX174 DNA. Nature (London) **265**: 687–695.
26. **Silverstein, S., R. Millette, P. Jones, and B. Roizman.** 1976. RNA synthesis in cells infected with herpes simplex virus. XII. Sequence complexity and properties of RNA differing in extent of adenylation. J. Virol. **18**: 977–991.
27. **Southern, E. M.** 1975. Detection of specific sequences among DNA fragments separated by gel electrophoresis. J. Mol. Biol. **98**:503–533.
28. **Stringer, J. R., L. E. Holland, R. I. Swanstrom, K. Pivo, and E. K. Wagner.** 1977. Quantitation of herpes simplex virus type 1 RNA in infected HeLa cells. J. Virol. **21**:889–901.
29. **Stringer, J. R., L. E. Holland, and E. K. Wagner.** 1978. Mapping early transcripts of herpes simplex virus type 1 by electron microscopy. J. Virol. **27**:56–73.
30. **Sutherland, B. M., M. Rice, and E. K. Wagner.** 1975. Xeroderma pigmentosum cells contain low levels of photoreactivating enzyme. Proc. Natl. Acad. Sci. U.S.A. **72**:103–107.
31. **Swanstrom, R. I., K. Pivo, and E. K. Wagner.** 1975. Restricted transcription of the herpes simplex virus genome occurring early after infection and in the presence of metabolic inhibitors. Virology **66**:140–150.
32. **Swanstrom, R., and P. R. Shank.** 1978. X-ray intensifying screens greatly enhance the detection by autoradiography of the radioactive isotopes ^{32}P and ^{125}I. Anal. Biochem. **86**:184–192.
33. **Swanstrom, R. I., and E. K. Wagner.** 1974. Regulation of synthesis of herpes simplex type 1 virus mRNA during productive infection. Virology **60**:522–533.
34. **Wadsworth, S., R. J. Jacob, and B. Roizman.** 1975. Anatomy of herpes simplex virus DNA. II. Size, composition, and arrangement of inverted terminal repetitions. J. Virol. **15**:1487–1497.
35. **Wagner, E. K., and B. Roizman.** 1969. RNA synthesis in cells infected with herpes simplex virus. II. Evidence that a class of viral mRNA is derived from a high molecular weight precursor synthesized in the nucleus. Proc. Natl. Acad. Sci. U.S.A. **64**:626–633.
36. **Wagner, E. K., R. I. Swanstrom, M. Rice, L. Howell, and J. Lane.** 1976. Variation in the molecular size of the DNA from closely related strains of type 1 herpes simplex virus. Biochim. Biophys. Acta **435**:192–205.
37. **Wagner, E. K., K. K. Tewari, R. Kolodner, and R. C. Warner.** 1974. The molecular size of the herpes simplex virus type 1 genome. Virology **57**:436–447.
38. **Watson, R. J., and J. B. Clements.** 1978. Characterization of transcription-deficient temperature-sensitive mutants of herpes simplex virus type 1. Virology **91**: 364–379.
39. **Wellauer, P. K., and I. B. Dawid.** 1973. Secondary structure maps of RNA: processing of HeLa ribosomal RNA. Proc. Natl. Acad. Sci. U.S.A. **70**:2827–2831.
40. **Wilkie, N. M., and R. Cortini.** 1976. Sequence arrangement in herpes simplex virus type 1 DNA: identification of terminal fragments in restriction endonuclease digests and evidence for inversions in redundant and unique sequences. J. Virol. **20**:211–221.